



Ballistic- and quantum-conductor carbon nanotubes: A reference experiment put to the test

M. Kobytko,^{1,2} M. Kociak,¹ Y. Sato,³ K. Urita,^{3,4} A. M. Bonnot,⁵ A. Kasumov,^{1,6} Y. Kasumov,⁶ K. Suenaga,³ and C. Colliex¹

¹Laboratoire de Physique des Solides (LPS), CNRS/Université Paris-Sud UMR 8502, Bâtiment 510, Orsay, France

²Laboratoire des Solides Irradiés (LSI), CEA/CNRS/Ecole Polytechnique UMR 7642, Ecole Polytechnique, Palaiseau, France

³Nanotube Research Center, National Institute of Advanced Industrial Science and Technology (AIST), Tsukuba, Japan

⁴Graduate School of Engineering, Nagasaki University, Nagasaki, Japan

⁵Institut Louis Néel, CNRS/UJF UPR 2940, BP 166, Grenoble, France

⁶Institute of Microelectronics Technology and High Purity Materials, Russian Academy of Sciences (IMT-RAS), Chernogolovka, Moscow Region, Russia

(Received 13 March 2014; published 20 November 2014)

We have performed electrical transport experiments on individual carbon nanotubes (CNTs) *in situ* in a transmission electron microscope using the liquid-metal contact method (LMC method), which consists of immersing a CNT placed on the apex of a metallic tip into a drop of liquid mercury (Hg). In the literature, this method has been mostly employed without visualization (*ex situ*) to show the ballistic- and quantum-conductance properties of different kinds of CNTs. We show that on the one hand the *in situ* LMC method is well suited to create low-resistance contacts with the CNTs but on the other hand the ballistic and quantum conductance measured by the *ex situ* LMC method is likely to give false positives for three reasons: (a) the CNTs are likely to be removed from the tip surface through contact with the Hg, (b) occurring Hg-tip surface nanocontacts are likely to be mistaken for quantum-conductor CNTs, and (c) occurring Hg nanomenisci are likely to be mistaken for ballistic-conductor CNTs. These findings have strong consequences for the interpretation of previously reported works.

DOI: [10.1103/PhysRevB.90.195431](https://doi.org/10.1103/PhysRevB.90.195431)

PACS number(s): 73.63.-b, 73.63.Fg

I. INTRODUCTION

Carbon nanotubes (CNTs), discovered by Iijima [1], are a fascinating material. Depending on their diameter and helicity, they can be conductors or semiconductors with different band gaps [2]. Thanks to these properties they have a high potential to become the building blocks of a new electronics at nanoscale [3]. Recently, an important milestone has been reached by Shulaker *et al.* [4], who constructed the first complete fully programmable CNT computer based alone on CNT field effect transistors (CNT-FETs) and thus proved the suitability of CNT-FET electronics for applications.

CNT-FET technology has the potential to become one order of magnitude more energy efficient than existing semiconductor technologies and thus to complement it in energy efficiency sensitive applications [5–8]. Notable technological achievements prior to the work of Shulaker *et al.* include the realization of CNT-FETs, logic gates, and stand-alone computational and storage circuit elements [9–14]. An important achievement is also the development of very large scale integration (VLSI) suitable fabrication methods which included overcoming challenges such as increasing the CNT-FET density and preventing logic device malfunction due to mispositioned and/or metallic CNTs within CNT-FETs [15–17].

However, electronic applications of CNTs so far have only been making use of the semiconducting (respectively metallic) nature of CNTs (and their resulting contact Schottky barriers) but not exploiting possible ballistic conduction or conductance quantification effects [2]. Thus, the continuous technological progress notwithstanding, the field of application of CNTs as nanoelectronics building blocks remains limited as long as their electrical transport properties are not sufficiently understood. As a striking example and due to the difficulty

of performing length-dependent conductivity measurements on well-characterized CNTs while limiting the influence of the environment (e.g., from the substrate), the question of whether multiwall CNTs (MWNTs) are ballistic [18,19] or diffusive conductors [20,21] has never been satisfactorily resolved.

One of the most important contributions in the debate on the ballistic or diffusive conduction in MWNTs is the famous experiment of Frank *et al.* [18] which showed (a) that MWNTs are room temperature ballistic conductors with electronic mean free paths (EMFPs) of several micrometers and (b) that the conductance of MWNTs is quantified in steps of $G = 1G_0 = 2e^2/h$ [instead of $G = 2G_0$ as predicted by theory [2] for single-wall CNTs (SWNTs)]. This experiment was performed by using an elegant liquid-metal contact method (LMC method) consisting of immersing the MWNTs placed on the apex of a metallic tip into a liquid metal [usually mercury (Hg)] and by supposing that in this way a mobile contact on the MWNT would be created [see Fig. 1(b)] which would allow one to measure the conductance versus length dependence of the immersed MWNT [see Figs. 1(a) and 1(c)].

This experiment has incited much similar work by several other groups [19,22–26] who considered the LMC method (or similar methods consisting of a cyclic immersion with no simultaneous visualization) also applicable on thin CNTs with micrometric lengths, i.e., single-wall CNTs (SWNTs) [23,25,26], double-wall CNTs (DWNTs) [22], and MWNTs [19,24] with a small number of walls. The interest of this kind of CNTs lies in their micrometric length which allows one to test micrometric EMFPs and in their limited wall number which facilitates the study of interwall interactions as well as in the unambiguous identification of their chiral indices by electron diffraction [27].

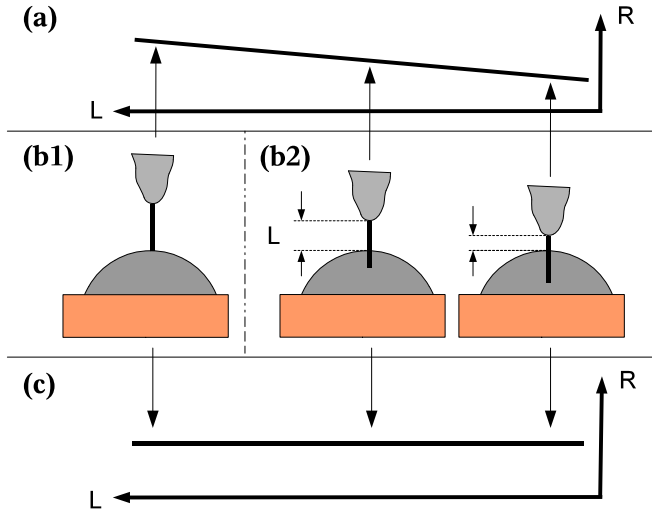


FIG. 1. (Color online) Illustration of the liquid-metal contact (LMC) method: (a) resistance-length dependence of diffusive CNTs, (b) schematic drawing of a CNT placed on a metallic tip being immersed into a drop of liquid metal, (c) resistance-length dependence of ballistic CNTs. In (b1), the resistance of the whole CNT is measured, whereas in (b2) only the resistance of the nonimmersed part of the CNT is measured. See text for more explanations.

In all these experiments, ballistic conductance was confirmed for the studied CNTs and EMPFs of the order of 10^{-6} m and even of the order of 10^{-5} m have been determined. Surprisingly, experiments performed with the liquid-metal method showed only once diffusive conduction of CNTs, namely by Poncharal *et al.* [28], and only on CNTs coated with a surfactant. To the best of our knowledge, diffusive conduction of pure CNTs has never been reported by groups using the liquid-metal contact or similar techniques, in contrast to other types of electrical transport experiments on individual CNTs [20,21].

In this paper, we first provide experimental evidence that (i) the *in situ* LMC method is well suited to create low-resistance contacts with CNTs and that (ii) the ballistic and quantum conductance measured by the *ex situ* LMC method is likely to give false positives for three reasons: (a) the CNTs are likely to be removed from the tip surface through contact with the Hg, (b) occurring Hg-tip surface nanocontacts are likely to be mistaken for quantum-conductor CNTs, and (c) occurring Hg nanomenisci are likely to be mistaken for ballistic-conductor CNTs. In consequence, many previous experimental results claiming ballistic and quantum conductance in CNTs have to be reinterpreted. By showing that the conductance measurements performed with the LMC method are likely to belong to other objects than CNTs (e.g., to Hg nanomenisci), this paper also helps to understand the experimental measurement of a $1G_0$ MWNT conductance in contradiction to the theoretical SWNT conductance of $2G_0$.

II. DESCRIPTION OF THE EXPERIMENT

We have performed several series of *in situ* transport experiments on individual thin CNTs (MWNTs with roughly five walls or less) using the Hg LMC method. Our CNTs

have been grown by two different CCVD methods using either Co/Ni [29] or Al/Fe catalysts [30] on nanometric tungsten (W) tips (obtained by electrochemical etching) and on AFM tips (metallized with a 20 nm thick Nb or Ti layer for better conduction).

The *in situ* transport experiments were performed inside a JEOL 2010F transmission electron microscope (TEM). We used two commercial nanomanipulator specimen holders: the JEOL EMZ8139T, which we combined with self-made electronics and software, and a Nanofactory [31] STM-TEM holder [32], suited with its own electronics and software. These *in situ* specimen holders allow electrical transport measurements with simultaneous visual information and mechanical control which is indispensable for this kind of experiment. Inside these specimen holders, the experimental geometry consists of two electrodes (one mobile, controlled by a piezoelectric ceramic, and one fixed) which face each other, one being the CNT-carrying tip and the other (the counterelectrode) a metallic tip carrying a Hg droplet (or in some of our experiments an Au tip). The apexes of both electrodes are in the field of view of the TEM.

III. EXPERIMENTAL RESULTS AND DISCUSSION

A. The *in situ* liquid-metal contact method is well suited to create low-resistance contacts with CNTs

The first part of our experimental study dealt with the question of whether the *in situ* LMC method (i.e., performed inside a TEM and thus with visualization) is well suited to create low-resistance contacts with CNTs in the configuration depicted in Fig. 1(b1), i.e., whether contacting the CNT with a liquid metal will result in a lower resistance contact than contacting it with a solid metal. Therefore, in some of our *in situ* experiments, we have replaced the Hg counterelectrode with an Au counterelectrode in order to measure the difference in the contact resistances between these two metals. We performed approximately 140 measurements on 9 CNTs brought into contact with Hg and 10 CNTs brought into contact with Au.

The resistance values were taken at low bias (0.1 V). Two sets of five tiplike samples as seen in Fig. 2 have been used respectively with the Au counterelectrode and the Hg counterelectrode. Three samples have been part of both sets, thereunder sample 1 and sample 2 referred to in Fig. 3 and Table I. Figure 3 shows histograms of the resistance

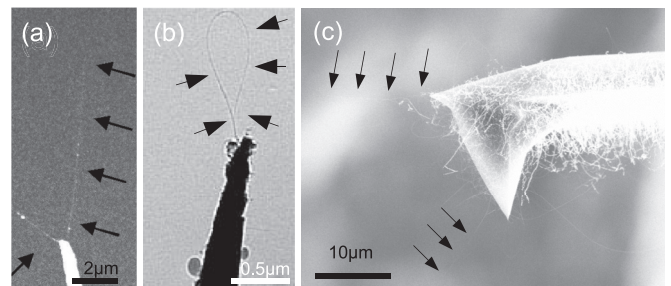


FIG. 2. CNTs on tips: (a) SEM image and (b) TEM image of CNTs on the apices of W tips, (c) SEM image of CNTs on the apex of an AFM tip.

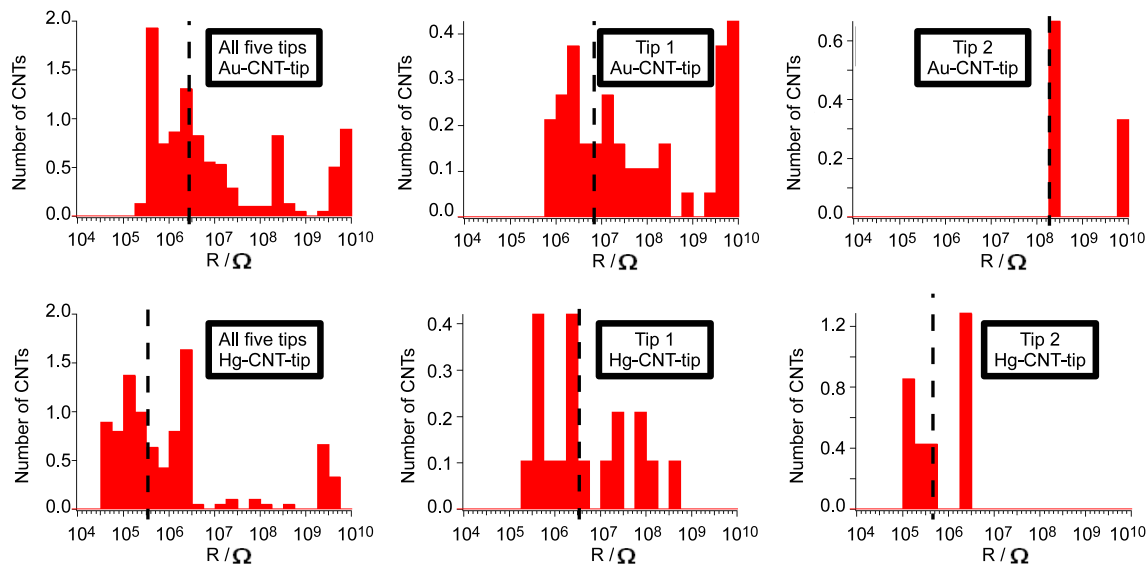


FIG. 3. (Color online) Histograms of Au/CNT-tip and Hg/CNT-tip low-bias contact resistance values. Note the logarithmic resistance scale. The area under the histograms gives the number of CNTs on the respective sample. Upper row: Au/CNT-tip resistance values. Lower row: Hg/CNT-tip resistance values. Left column: Resistance values for all five samples taken on 10 CNTs (for Au) respectively 9 CNTs (for Hg) in contact with different places on the Au (respectively Hg) counterelectrode. Middle column: Resistance values for sample 1 taken on 3 CNTs (for Au) respectively on 2 CNTs (for Hg) in contact with different places on the Au (respectively Hg) counterelectrode. Right column: Resistance values for sample 2 taken on 1 CNT (for Au) respectively on 3 CNTs (for Hg) in contact with different places on the Au (respectively Hg) counterelectrode. Dashed lines indicate the positions of the geometrical average resistances. Resistance values above 1 G Ω have not been considered in the calculation of the geometrical average resistances.

values for sample 1, for sample 2, and for all samples. These histograms of subsequent conductivity measurements have been normalized in such a way as to give each CNT the same statistical weight, taking into account that the number of conductivity measurements performed on each CNT differed between different CNTs. Hence, the area under the histograms is equal to the number of CNTs on the respective sample. The legend of Fig. 3 gives further information. Resistance values above 1 G Ω are not trustworthy because our measurement system has a leakage-current-induced detection limit between 1 G Ω and 10 G Ω .

TABLE I. Comparison of Au/CNT-tip and Hg/CNT-tip low-bias contact resistance values. Left column: Geometrical average resistance of 10 CNTs (for Au) respectively 9 CNTs (for Hg) mounted on five different tips in contact with different places on the Au respectively Hg counterelectrode. Middle column: Geometrical average resistance of 3 CNTs (for Au) respectively 2 CNTs (for Hg) mounted on tip 1 in contact with different places on the Au respectively Hg counterelectrode. Right column: Geometrical average resistance of 1 CNT (for Au) respectively 3 CNTs (for Hg) mounted on tip 2 in contact with different places on the Au respectively Hg counterelectrode. Last row: Ratio of the respective Au/CNT-tip contact resistance to the Hg/CNT-tip contact resistance.

	$\overline{R}_{\text{total}}/\Omega$	\overline{R}_1/Ω	\overline{R}_2/Ω
Au	2.7×10^6	6.8×10^6	1.8×10^8
Hg	3.3×10^5	3.4×10^6	4.4×10^5
Ratio	8.2	2.0	4.1×10^2

One notices that the resistances values in Fig. 3 are widely distributed which shows that the contact resistance value depends strongly on the place where the CNT touches the Au or Hg counterelectrode. One sees that the distributions of the Hg/CNT-tip low-bias contact resistances are shifted to the left in comparison to the respective distribution of the Au/CNT-tip low-bias contact resistances. This shift can be analyzed in several ways. First, one can look on the minimum resistances which are approximately 40 k Ω [= 1/(0.3 G_0)] for a Hg/CNT-tip system and approximately 250 k Ω [= 1/(0.05 G_0)] for a Au/CNT-tip system. Second, one can compare the peaks which dominate the resistance distributions. These are approximately 400 k Ω , approximately 2 M Ω , and approximately 200 M Ω for the Au/CNT-tip systems and approximately 100 k Ω and approximately 2 M Ω for the Hg/CNT-tip systems. Third, one can compare the average resistance values. Due to the wide distribution of the resistance values spanning several orders of magnitude, geometrical averages are more appropriate than arithmetic averages. Thus, the geometrical average resistances have been calculated according to Eq. (1):

$$\overline{R} = 10^{(\sum_{i=1}^n \log_{10} R_i)/n}. \quad (1)$$

As they are not trustworthy, the resistance values above 1 G Ω have not been considered in the calculation of the geometrical average resistances. The geometrical average resistances are indicated in Fig. 3 as dashed lines. Their numerical values are shown in Table I. For sample 1, the geometrical average Hg/CNT-tip resistance is approximately 2 times smaller than the geometrical average Au/CNT-tip resistance. For sample 2, the geometrical average Hg/CNT-tip resistance is approximately 4.1×10^2 times smaller than the

geometrical average Au/CNT-tip resistance. In total, the geometrical average Hg/CNT-tip resistance is 8.2 times smaller than the geometrical average Au/CNT-tip resistance. Fourth, one can compare not only the histograms in which each CNT has the same statistical weight as in Fig. 3, but also histograms in which each sample has the same statistical weight (not shown), or in which each measurement has the same statistical weight (not shown). Those results are qualitatively the same as these shown here.

In conclusion, the minimum resistances we have measured *in situ* at low bias were approximately 40 k Ω [= 1/(0.3 G_0)] for a Hg/CNT-tip system and approximately 250 k Ω [= 1/(0.05 G_0)] for an Au/CNT-tip system. Independently of the statistical analysis technique, our results show clearly that Hg-CNT contacts are on average between three and ten times less resistive at low bias than Au-CNT contacts. Therefore we conclude that the *in situ* LMC method (i.e., performed in a TEM and thus with visualization) is well suited to create low-resistance contacts with the CNTs and, in consequence, also to measure the total conductance of the non-Hg-immersed part of the CNT in the configuration depicted in Fig. 1(b1).

B. The ballistic- and quantum-conductance measurement by the *ex situ* LMC method is likely to give false positives

The second part of our experimental study dealt with the question of whether the *ex situ* LMC method (i.e., not performed in a TEM and thus without visualization) is reliable in the two configurations (b1) and (b2) depicted in Fig. 1. For the LMC method to be reliable *ex situ*, it is important that the measured conductance can only be the conductance of the CNT and of nothing else. In the following, we will show by means of *in situ* LMC experiments that this necessary condition is not fulfilled.

1. The LMC method with simultaneous *in situ* visualization

In Fig. 4, we show the results of an *in situ* experiment realized using the common experimental protocol for *ex situ* experiments involving cyclic immersion of CNTs into the Hg and the representation of the measured conductance values in a histogram. Figure 4 shows the conductance vs time dependence while a sinusoidal voltage is applied to the piezoelectric ceramic. The conductance does not change in a continuous way (as would be the case for a diffusive conductor) but forms well-defined stable plateaus over up to about 300 nm length. We see that the conductance takes a higher value when the Hg meniscus touches a bigger part of the tip surface (right part of Fig. 4).

According to the criteria suggested in the original work of Frank *et al.* [18] and subsequently accepted in the literature [19,22–26], the same experimental results (if acquired in an *ex situ* experiment without visual control) would show that the CNT at the apex of the tip is a ballistic conductor (due to the stability of the plateaus) and that its conductance is quantified (due to the appearance of peaks in the histogram). One can therefore define a quantification step G_1 which is the conductance value of which the total measured conductance appears to always be an integer multiple. In the picture adopted by Frank *et al.* [18], G_1 would thus correspond to the conductance of a single CNT and measuring multiples

of G_1 would signify that several CNTs are immersed in the Hg at the same time. The value of G_1 can be deduced from the histogram (see right side of Fig. 4). However, in the data set we show G_1 cannot be determined unambiguously due to the presence of only two peaks and its broadness. Two (mutually exclusive) values of G_1 are indeed possible. First, the quantification step G_1 could be $G_1 = 2.5 \dots 3G_0$ in which case the left two plateaus of Fig. 4 would correspond to a conductance of $G = 1G_1$ and the right two plateaus of Fig. 4 to a conductance of $G = 2G_1$. Second, the quantification step G_1 could be $G_1 = 1.0G_0$ in which case the left two plateaus of Fig. 4 would correspond to a conductance of $G = 3G_1$ and the right two plateaus of Fig. 4 to a conductance of $G = 5G_1$. However, for our present study it is not the precise value of G_1 which is important but rather the fact that the value of G_1 is close to conductance quantum G_0 which has been identified as the quantification step of CNTs by Frank *et al.* [18]. Figure 4 thus unambiguously shows that the *ex situ* LMC method is likely to give false positives of ballistic transport properties, of conductance quantification, and of the conductance quantification step value. Note that the here presented histogram (despite showing only two peaks of which one is broadened) is nonetheless comparable to those from which conductance quantification of CNTs has been concluded [18,33] as those were similarly broadened and sometimes did not even show two peaks as here but rather as little as one single peak.

2. Reasons for the unreliability of the *ex situ* LMC method

Figure 4 demonstrates that a measurement equivalent to that of Frank *et al.* [18] can be obtained without even a CNT present. In this section, we point out how this fact makes the LMC method unreliable in an *ex situ* experiment without simultaneous visualization.

The first reason is that (as we could observe in our *in situ* experiments) the CNTs on the tip surface are likely to be removed through contact with the Hg. The experimental *in situ* setup permitted us to visualize CNTs immediately before and immediately after an immersion into the Hg. Poncharal *et al.* [34] have already observed a cleansing effect of the Hg on the sample in low-magnification *in situ* experiments: removing graphitic particles and poorly connected CNTs by the Hg. In our higher magnification *in situ* experiments we could see this effect more precisely (see Figs. S1 and S2 in the Supplemental Material [35] for two examples): after a Hg immersion, we often saw CNTs move, break, or disappear. Moving the CNTs can make them stick together or fall apart. The Hg also moves clusters of metallic and graphitic particles and sometimes deposits them on the CNTs. Sometimes, a Hg immersion can even remove parts of the tip surface layer together with the CNTs located on it. Thus, even if it is not always the case, already a number of Hg immersions as small as five has often a devastating effect on the CNTs at the apex. We conclude from this observation that, in general, a removal of the CNTs by the Hg (and thus the creation of an experimental configuration analogous to that depicted in Fig. 4) during *ex situ* experiments involving hundreds or thousands of Hg immersions (like in the original work of Frank *et al.* [18]) is extremely likely.

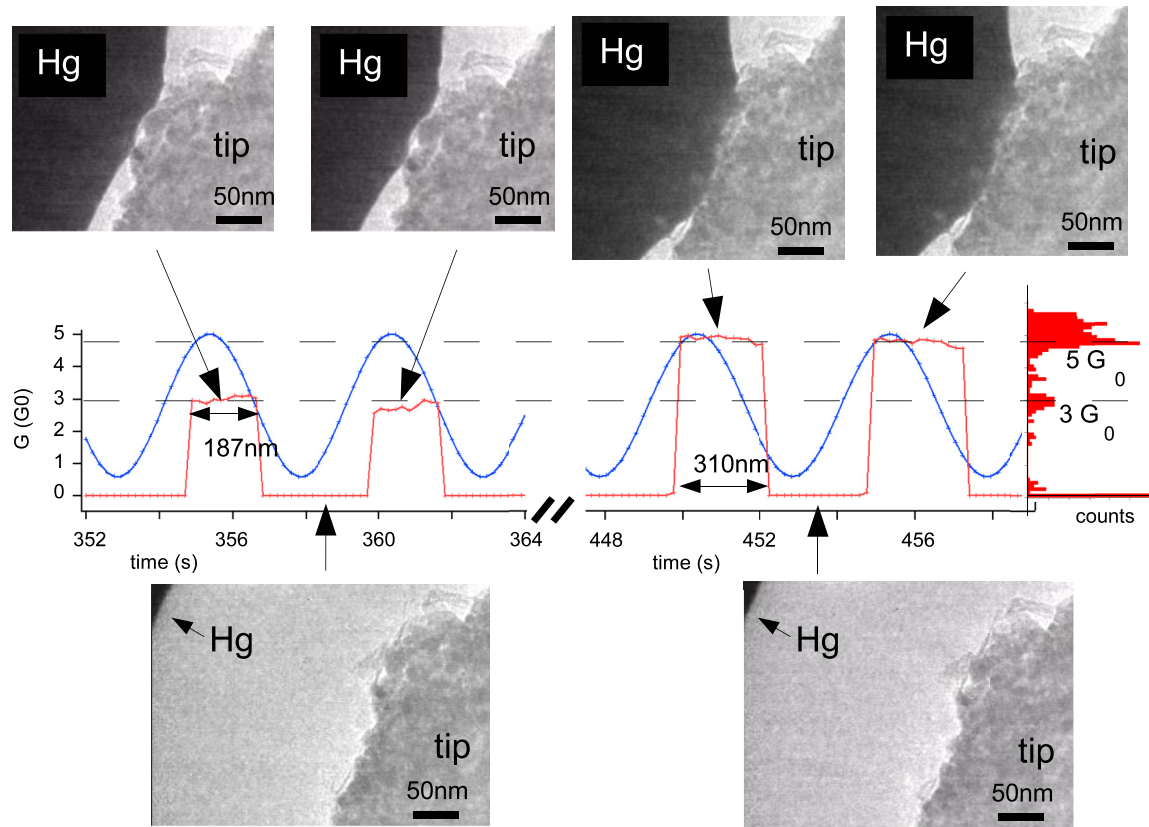


FIG. 4. (Color online) Upper part: the conductance vs time dependence, acquired *in situ* during cyclic immersion of a tip with CNTs at the apex into the Hg according to the common experimental protocol for *ex situ* experiments, meets the criteria for ballistic transport and conductance quantification [red: conductance, blue: sample displacement (amplitude: 220 nm)]; lower part: only visual control can tell us that the transport measurement is not being performed on CNTs but on several Hg nanomenisci sticking to the tip surface, the CNTs having been removed by the Hg during previous immersions. The length of the conductance plateaus as expressed in nm is defined as the position of the sample at the beginning of the plateau minus the position of the sample at the end of the plateau.

The second reason is that (in an experimental configuration without CNTs) Hg menisci are likely to be mistaken for ballistic conductors. The reason for that is that (as observed in our *in situ* experiments) they follow the mechanical movement of the (previously CNT-carrying) tip over hundreds of nanometers and that (as also observed in our *in situ* experiments) their conductance does not depend on their length. (The last point indicates that it is rather the resistance of the Hg-tip contact that we measure rather than the resistance of the Hg meniscus. This point will be discussed in Sec. III C.) These two observations are already shown in Fig. 4 in a dynamical setting (periodically oscillating mechanical displacement). Figure 5 confirms these observations in a more static setting. It shows a Hg meniscus sticking to a tip apex carrying no CNTs. During retraction and approach of the tip to the Hg droplet of about 100 nm, the Hg meniscus follows the tip. Note that a tip displacement of about 100 nm is not unusually short for *ex situ* experiments carried out with the liquid-metal contact method [18]. During this mechanical manipulation, the conductance varies but the variation is uncorrelated to the mechanical displacement. In addition, the value of the conductance is between $0.5G_0$ and $1G_0$ which is very close to the conductance value of $1G_0$ which has been assigned by Frank *et al.* [18] to ballistic CNTs. Such experimental results, if acquired in an *ex situ* experiment

without visual control, would be likely to suggest a ballistic CNT at the apex of the tip (in particular at the much shorter time scales and the dynamical setting used in the original work of Frank *et al.* [18], which would not make the conductance variation as apparent as in the static setting of Fig. 5). In reality, there is not even a CNT present, and one measures only the conductance of the Hg meniscus which follows the tip.

The third reason is that Hg/tip-surface nanocontacts are likely to be mistaken for CNTs in an *ex situ* LMC experiment, as they are likely to have conductance values close to the conductance quantum G_0 (see Fig. 4 and Fig. 5). In Sec. III C, the origin of this conductance value is discussed.

Due to the three above-mentioned reasons, one can assure the presence of CNTs on the apex of the tip and the correct interpretation of the experimental results only by simultaneous *in situ* visualization. In Fig. 4, no CNT is present at the tip of the sample due to before-mentioned removal of the CNTs during previous Hg immersions. Instead of the CNT conductance, we measure the conductance of the Hg nanocones and the tip surface covered by catalytic particles and graphitic layers. The illusion of ballistic transport arises from the fact that the Hg meniscus follows the retracting tip and that the conductance is most likely determined by the Hg-tip contact rather than the

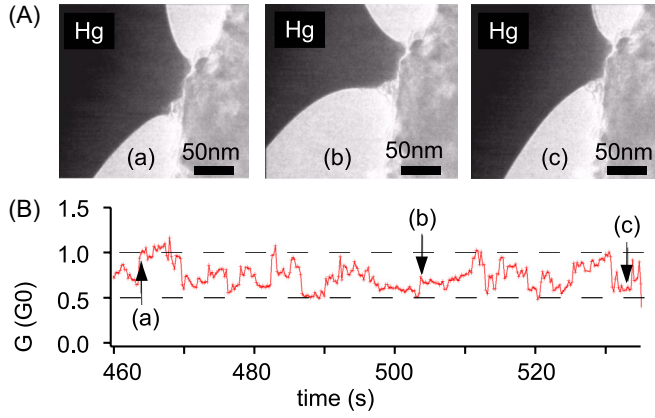


FIG. 5. (Color online) A Hg meniscus sticking to the apex of the tip. (A) Visualization. (B) Conductance vs time dependence. (a), (b), and (c) designate the moments in (B) at which the corresponding images in (A) were taken. The sample displacement between (a) and (b), and between (b) and (c), is monotonic. During retraction and approach of the tip to the Hg droplet of about 100 nm, the Hg meniscus follows the tip. The conductance varies but the variation is uncorrelated to the mechanical displacement.

conductance of the Hg meniscus itself. The fact that at almost each Hg immersion the same kind of contact as at the previous immersion is formed, and that the same contact has always the same conductance, is responsible for the occurrence of peaks in the conductance histogram. The existence of a conductance value G_1 , on whose multiples these peaks are centered, creates the illusion of quantification of conductance in steps of G_1 .

As confirmed by our *in situ* observations, Fig. 4 depicts a scenario which is extremely likely to happen (but impossible to detect) in *ex situ* LMC experiments (i.e., without simultaneous visualization) on CNT-carrying tips, in particular in the oscillating and highly repetitive conditions (hundreds to thousands of oscillations) of the experiments of Frank *et al.* [18] and similar work [19,22–24]. Therefore, the *ex situ* LMC method must be considered unreliable in both configurations (b1) and (b2) depicted in Fig. 1.

C. Origin of the measured quantum conductance

In addition to showing the unreliability of the liquid-metal contact method, our *in situ* experiments show that the conductance of a Hg nanomeniscus contacted to the tip surface across catalytic and graphitic particles can be close to the quantum conductance G_0 . In order to answer the question if this conductance value can be attributed to the Hg nanomeniscus itself, we estimated its expected conductance value in two different ways. First, we estimated the conductance of three Hg nanomenisci shown in Figs. 5 and 4 using the classical macroscopic concept of resistivity. From the definition of resistivity ρ , one can easily deduce Eq. (2) for the classical conductance G_{class} of a homogenous cone with the smaller radius r_1 , the bigger radius r_2 , and the length L :

$$G_{\text{class}} = \frac{\pi r_1 r_2}{\rho L}. \quad (2)$$

These so calculated conductance values of the Hg nanomenisci, shown in Table II, are between 10^2 and 10^4 times the measured ones. Second, we estimated the conductance of the same Hg nanomenisci by assuming them to be narrow ballistic quantum conductors with a limited number of transverse electronic modes. The Fermi wavelength λ_F of Hg has been roughly approximated with the free-electron-model value [36] $\lambda_F = [(8\pi)/(3n)]^{1/3}$ (n being the number of electrons per volume unit which gives $\lambda_F = 0.47$ nm for Hg). According to Datta [37], the rough number M_{trans} of the transverse electronic modes in a narrow cylinder with the radius r_1 and the length L is given by Eq. (3) ($\lfloor x \rfloor$ being the biggest integer which is not bigger than x):

$$M_{\text{trans}} = \left\lfloor \frac{\pi r_1^2}{(\lambda_F/2)^2} \right\rfloor. \quad (3)$$

The conductance G_{quant} of a ballistic quantum conductor with this number of modes is then simply given by Eq. (4) [37]:

$$G_{\text{quant}} = G_0 M_{\text{trans}}. \quad (4)$$

These so calculated conductance values of the Hg nanomenisci, shown in Table II, are between 10^3 and 10^5 times the measured ones. As the quantum-conductor estimation delivers values at least one order of magnitude higher than the classical estimation, one usually would conclude that these Hg nanomenisci should theoretically behave as classical conductors. However, regardless of whether we assume them to be classical conductors or to be quantum conductors, the estimated resistance values of the Hg nanomenisci are several orders of magnitude lower than the measured ones. Hence, we conclude that the measured resistance cannot come from the Hg nanomenisci if these can be described either as classical conductors with the same resistivity as bulk Hg or as narrow ballistic conductors with the same transverse electronic mode density as bulk Hg. We rather suppose that the tip-surface-covering layer of catalytic particles and graphite is not homogeneously conducting and that the measured resistance of the Hg nanomenisci could potentially be attributed to the percolation resistance of this layer.

This hypothesis is supported by the experimental observation of forty different Hg nanomenisci sticking to about ten different places on the tip and the measurement of their conductance. Figure 6 shows some examples of these Hg nanomenisci with their respective conductance values. The Hg nanomenisci sticking to the same place nearly always had the same conductance. Where occasionally this was not the case, we attribute this to a slight change of the sticking surface whose exact observation is impossible for geometrical reasons. In contrast, comparable Hg nanomenisci sticking to different places had very different conductance values. For about half of the sticking places the conductance was ranging from $0.3G_0$ to $3.0G_0$, however always staying of the order of G_0 ; for the other half the conductance was $0G_0$. We therefore assume that only a randomly distributed fraction of the tip-surface covering layer of our samples is conductive leading to a percolation type of conductance and that the conductance of a Hg-nanomeniscus-to-tip contact depends among others on how many of these conductive spots the Hg nanomeniscus touches. We also conclude that, contrary to expectations, direct

TABLE II. Smaller radius, bigger radius, length, classically estimated, quantally estimated, and experimentally measured conductance of different Hg menisci. (Especially for Fig. 4, the geometrical values are very imprecise and should be rather understood in terms of orders of magnitude.)

Meniscus	r_1/nm	r_2/nm	L/nm	G_{class}/G_0	G_{quant}/G_0	G_{exp}/G_0
Fig. 5 (middle)	25	25	50	~ 530	~ 36000	$0.5 \dots 1.0$
Fig. 4 (left)	10	30	10	~ 1300	~ 5700	3
Fig. 4 (right)	150	250	30	~ 53000	~ 1300000	5

CCVD growth of CNTs on metal samples does not necessarily result in low-resistance contacts.

D. Is the *in situ* LMC method suited to measure the conductance-length dependence of CNTs?

In addition to the question of whether the *ex situ* LMC method is reliable, we have also investigated whether the *in situ* LMC method is suited to measure the conductance-length dependence of CNTs in the configuration depicted in Fig. 1(b2) if one manages to rule out the possibility of the removal of the CNTs from the tip surface and the measurement of the Hg nanomenisci and nanocontacts (instead of the CNT) in a specially designed *in situ* experiment. Note that proof for ballistic and quantum conductance in CNTs from such experiments has to our best knowledge never been reported.

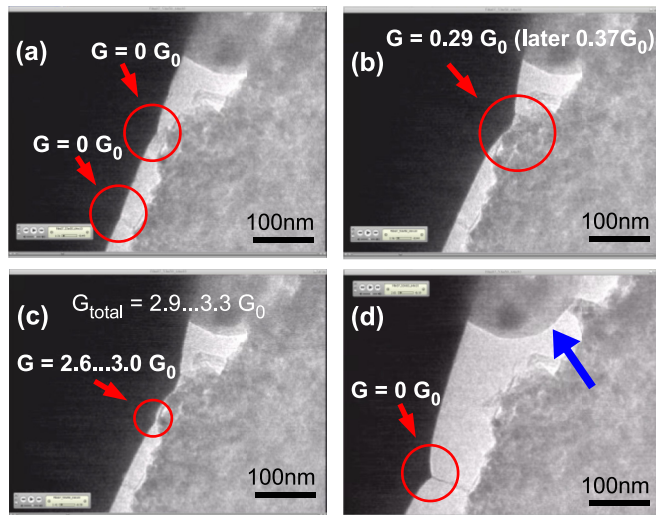


FIG. 6. (Color online) Examples of Hg nanomenisci sticking to different places on the tip surface (Hg: black contrast, upper left corner; tip: dark gray contrast, lower right corner) shown in chronological order. Only the maximum values of each contact conductance are taken into account. The conductance values of new small nanocontacts (red circles) are calculated as the difference between two consecutive total conductance values of the Hg nanomenisci. These nanocontact conductance values are always either $0G_0$ or of the order of G_0 . In particular, image (d) proves that the conductance of a CNT in contact with the Hg droplet can be $0G_0$. Also shown is a particle (diameter > 200 nm), which does not make mechanical contact with the tip surface as it is at a different height. This particle is floating on the Hg surface (thick blue arrow) and has been most likely detached from the tip surface by a Hg immersion.

In the original paper of Frank *et al.* [18], Fig. 1 shows only a TEM image of the CNT-carrying tip whereas Fig. 2 shows conductivity-length dependence curves acquired in an *ex situ* scanning probe microscope (SPM) experiment without visualization (thus without certainty that it is the conductance of CNTs which is measured). This equally holds true for the subsequent papers [28,34,38,39]. In the work of Wang *et al.* [38], *in situ* experiments have been performed but any conductivity-length dependence curves possibly acquired in these experiments are not shown. Figure 3 of Wang *et al.* [38] shows an image of an *in situ* TEM transport experiment (however without a conductivity-length dependence) whereas Fig. 4 of Wang *et al.* [38] shows the conductivity-length dependence acquired in an *independent ex situ* atomic force microscope (AFM) experiment (without visualization, thus without certainty that it is the conductance of CNTs which is measured). In the work of Poncharal *et al.* [34], Fig. 1 shows a conductivity-length dependence curve acquired in an *in situ* experiment; however TEM images possibly acquired simultaneously with these electrical measurements are not shown, and thus it remains impossible to ascertain whether these conductance can be attributed to CNTs or not. In a subsequent paper of Poncharal *et al.* [28], Fig. 1(a) shows an image of an *in situ* TEM transport experiment (however without a conductivity-length dependence) whereas Fig. 1(b) shows the conductivity-length dependence acquired in an *independent ex situ* SPM experiment (without visualization, thus without certainty that it is the conductance of CNTs which is measured). Further in the same paper of Poncharal *et al.* [28], Figs. 2(d) and 2(e) only show TEM images of the CNT-carrying tip before and after transport measurements whereas Figs. 2(a)–2(c) show conductance-length dependence curves acquired in an *ex situ* SPM experiment (without visualization, thus again without certainty that it is the conductance of CNTs which is measured). It is true that Fig. 2(e) confirms that a small number of CNTs (or small CNT bundles which cannot be decided due to the insufficient magnification and resolution of the TEM image) out of a high initial number of CNTs or CNT bundles has survived the cyclic immersion process. Nonetheless, this fact alone is not sufficient to confirm that the conductance plateaus in Fig. 2(c) can really be attributed to the CNTs. Rather, it is much more likely that these conductance plateaus are due to Hg menisci as we argue in this paper. Poncharal *et al.* [28] even support our argument by showing a TEM image of a Hg meniscus sticking to the end of a CNT in Fig. 1(a). Further in the same paper of Poncharal *et al.* [28], Figs. 3–6 show conductance measurements from *ex situ* SPM experiments (without visualization), Fig. 7 *in situ* TEM observations without conductance-length dependence curves,

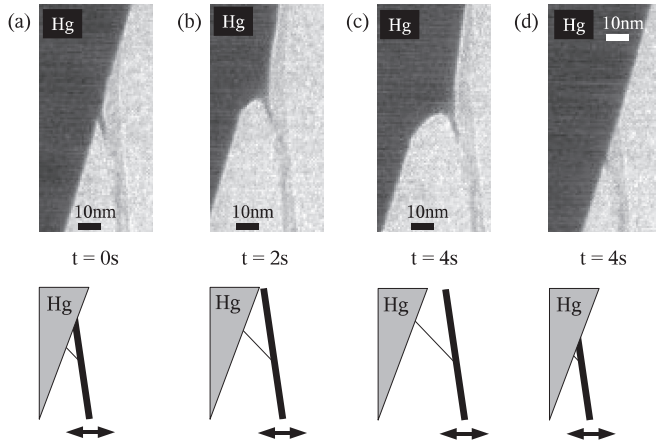


FIG. 7. A CNT rope which bifurcates close to the Hg surface. A thin part of the rope is in contact with a Hg meniscus which appears to be strongly pinned to it and which follows the CNT rope during its retraction from and approach to the Hg droplet of about 30 nm. However, the majority of the CNTs inside the rope lie down on the Hg surface.

and Fig. 11 conductance value histograms from experiments on gold nanowires and not from experiments on CNTs. Another paper using the LMC method (Berger *et al.* [39]) does not show any conductance-length dependence curves at all, either from *in situ* or *ex situ* experiments. In addition to the above remarks, no conductance-length dependence curves corresponding to cyclic immersion *in situ* TEM experiments and no corresponding conductance value histograms are shown in any of the above papers [28,34,38,39].

As the nonexistence of successful conductance-length dependence measurements by the *in situ* LMC method does not exclude that such an experiment might be in principle possible, we chose a different approach in order to investigate this question: in order to investigate whether the *in situ* LMC method is suited to measure the conductance-length dependence of CNTs in the configuration depicted in Fig. 1(b2) if one manages to rule out the possibility of the removal of the CNTs from the tip surface and the measurement of the Hg nanomenisci and nanocontacts (instead of the CNT) in a specially designed *in situ* experiment, we have performed numerical simulations based on an analytical mechanical model of the CNT-Hg immersion process.

The analytical model (published separately [40]) assumes that a mobile contact on the CNT can be created in two ways: either by the CNT penetrating the Hg surface or by the CNT lying down on the Hg surface (see Fig. 7 for an example). Simulations based on the above analytical model show that most CNTs will not create a mobile contact with the Hg surface under realistic experimental conditions. (Especially, the most interesting objects, SWNTs and DWNTs with micrometric lengths and arbitrary diameters, will not create a mobile contact with the Hg even for experimentally unattainably small deviation angles.) In addition, the small minority of CNTs which will create a mobile contact will not behave as expected either: From the moment at which the tip of the CNT touches the Hg surface until the moment at which the tip of the CNT moves under the Hg surface or lies down on it, the

CNT-carrying sample will have to be approached by a certain distance to the Hg surface. This distance will be a systematic error on the electronic mean free path (EMFP) of the CNTs one tries to determine by these experiments and can be up to 100% of the measured value.

IV. CONCLUSION

In conclusion, our experimental results show that the *in situ* LMC method (i.e., performed inside a TEM and thus with visualization) is well suited to create low-resistance contacts with the tip of the CNT in the configuration depicted in Fig. 1(b1) and therefore also to measure the conductance of the whole CNT. However, our *in situ* experiments also prove that the ballistic and quantum conductance measured by the *ex situ* LMC method (i.e., not performed in a TEM and thus without visualization) in both configurations (b1) and (b2) depicted in Fig. 1 is likely to give false positives for three reasons: (a) the CNTs are likely to be removed from the tip surface through contact with the Hg, (b) occurring Hg/tip-surface nanocontacts are likely to be mistaken for quantum-conductor CNTs, and (c) occurring Hg nanomenisci are likely to be mistaken for ballistic-conductor CNTs. As these possibilities cannot be ruled out in an *ex situ* LMC experiment, the results obtained by this method have to be interpreted with great caution keeping in mind that they are very likely measurements on other objects than CNTs. (It is also for this reason that only the *in situ* LMC method—and not the *ex situ* LMC method—is suited to measure the conductance of the whole CNT.) In consequence, many previous experimental results claiming ballistic and quantum conductance in CNTs have to be reinterpreted.

In situ experiments and numerical simulations based on an analytical mechanical model of the CNT-Hg immersion process (published separately [40]) show that not only the *ex situ* but also the *in situ* LMC method is unsuitable for ballistic- and quantum-conductance measurements on CNTs in the configuration depicted in Fig. 1(b2). The reason is that most CNTs will not create a mobile contact with the Hg surface under realistic experimental conditions, and that the rest of the CNTs will have a systematic error on the measurement of its mean free path of up to 100% of the measured value.

Finally, our experiments have shown that Hg-tip nanocontacts between a Hg droplet and a tip covered by a CCVD residue layer of disordered graphitic and metallic particles can have a conductance close to the conductance quantum G_0 which cannot be explained either by a simple classical or by a simple quantum model. Their conductance values are reproducible and depend on the precise location at which the Hg nanomeniscus touches the tip surface. A possible explanation could be an inhomogeneous conductivity of the CCVD residue layer leading to a percolation-type conductance.

In conclusion, these experimental results show that the *ex situ* LMC method is not reliable for ballistic- and quantum-conductance measurements on CNTs. This work challenges previously published and accepted results and we hope that it will help to resolve the controversy about the ballistic and diffusive nature of CNTs.

- [1] S. Iijima, *Nature (London)* **354**, 56 (1991).
- [2] R. Saito, G. Dresselhaus, and M. Dresselhaus, *Physical Properties of Carbon Nanotubes* (Imperial College Press, London, 1998).
- [3] W. Hoenlein, G. S. Duesberg, A. P. Graham, F. Kreupl, M. Liebau, W. Pamler, R. Seidel, and E. Unger, *Microelectron. Eng.* **83**, 619 (2006).
- [4] M. M. Shulaker, G. Hills, N. Patil, H. Wei, H.-Y. Chen, H. S. Philip Wong, and S. Mitra, *Nature (London)* **501**, 526 (2013).
- [5] D. E. Nikonov and I. A. Young, *Proc. IEEE* **101**, 2498 (2013).
- [6] D. E. Nikonov and I. A. Young, *IEEE Int. Electron Devices Meet.* **2012**, 25.4.1.
- [7] A. D. Franklin, M. Luisier, S.-J. Han, G. Tulevski, C. M. Breslin, L. Gignac, M. S. Lundstrom, and W. Haensch, *Nano Lett.* **12**, 758 (2012).
- [8] L. Wei, D. J. Frank, L. Chang, and H.-S. P. Wong, *IEEE Int. Electron Devices Meet.* **2009**, 1.
- [9] R. Martel, T. Schmidt, H. R. Shea, T. Hertel, and P. Avouris, *Appl. Phys. Lett.* **73**, 2447 (1998).
- [10] S. J. Tans, A. R. M. Verschueren, and C. Dekker, *Nature (London)* **393**, 49 (1998).
- [11] A. Bachtold, P. Hadley, T. Nakanishi, and C. Dekker, *Science* **294**, 1317 (2001).
- [12] Z. H. Chen, J. Appenzeller, Y. M. Lin, J. Sippel-Oakley, A. G. Rinzler, J. Y. Tang, S. J. Wind, P. M. Solomon, and P. Avouris, *Science* **311**, 1735 (2006).
- [13] Q. Cao, H.-s. Kim, N. Pimparkar, J. P. Kulkarni, C. Wang, M. Shim, K. Roy, M. A. Alam, and J. A. Rogers, *Nature (London)* **454**, 495 (2008).
- [14] N. Patil, A. Lin, J. J. Zhang, H. Wei, K. Anderson, H. S. P. Wong, and S. Mitra, *IEEE Trans. Nanotechnol.* **10**, 744 (2011).
- [15] Q. Cao, S.-j. Han, G. S. Tulevski, Y. Zhu, D. D. Lu, and W. Haensch, *Nat. Nanotechnol.* **8**, 180 (2013).
- [16] J. Zhang, A. Lin, N. Patil, H. Wei, L. Wei, H. S. P. Wong, and S. Mitra, *IEEE Trans. CAD* **31**, 453 (2012).
- [17] M. M. Shulaker, H. Wei, N. Patil, J. Provine, H.-Y. Chen, H. S. P. Wong, and S. Mitra, *Nano Lett.* **11**, 1881 (2011).
- [18] S. Frank, P. Poncharal, Z. L. Wang, and W. A. de Heer, *Science* **280**, 1744 (1998).
- [19] A. Urbina, I. Echeverria, A. Perez-Garrido, A. Diaz-Sanchez, and J. Abellan, *Phys. Rev. Lett.* **90**, 106603 (2003).
- [20] L. Langer, V. Bayot, E. Grivei, J. P. Issi, J. P. Heremans, C. H. Olk, L. Stockman, C. Van Haesendonck, and Y. Bruynseraede, *Phys. Rev. Lett.* **76**, 479 (1996).
- [21] A. Bachtold, C. Strunk, J. P. Salvetat, J. M. Bonard, L. Forro, T. Nussbaumer, and C. Schonenberger, *Nature (London)* **397**, 673 (1999).
- [22] H. Kajiura, H. J. Huang, and A. Bezryadin, *Chem. Phys. Lett.* **398**, 476 (2004).
- [23] H. Kajiura, A. Nandyala, U. C. Coskun, A. Bezryadin, M. Shiraishi, and M. Ata, *Appl. Phys. Lett.* **86**, 122106 (2005).
- [24] H. Kajiura, A. Nandyala, and A. Bezryadin, *Carbon* **43**, 1317 (2005).
- [25] N. R. Wilson, D. H. Cobden, and J. V. Macpherson, *J. Phys. Chem. B* **106**, 13102 (2002).
- [26] J. Y. Chen, A. Kutana, C. P. Collier, and K. P. Giapis, *Science* **310**, 1480 (2005).
- [27] M. Kociak, K. Hirahara, K. Suenaga, and S. Iijima, *Eur. Phys. J. B* **32**, 457 (2003).
- [28] P. Poncharal, C. Berger, Y. Yi, Z. L. Wang, and W. A. de Heer, *J. Phys. Chem. B* **106**, 12104 (2002).
- [29] L. Marty, A. Iaia, M. Faucher, V. Bouchiat, C. Naud, M. Chaumont, T. Fournier, and A. M. Bonnot, *Thin Solid Films* **501**, 299 (2006).
- [30] Y. A. Kasumov, A. Shailos, I. I. Khodos, V. T. Volkov, V. I. Levashov, V. N. Matveev, S. Gueron, M. Kobylyko, M. Kociak, H. Bouchiat, V. Agache, A. S. Rollier, L. Buchaillot, A. M. Bonnot, and A. Y. Kasumov, *Appl. Phys. A* **88**, 687 (2007).
- [31] Nanofactory Instruments AB, Göteborg, Sweden.
- [32] K. Svensson, Y. Jompol, H. Olin, and E. Olsson, *Rev. Sci. Instrum.* **74**, 4945 (2003).
- [33] N. Agrait, A. L. Yeyati, and J. M. van Ruitenbeek, *Phys. Rep.* **377**, 81 (2003).
- [34] P. Poncharal, S. Frank, Z. L. Wang, and W. A. de Heer, *Eur. Phys. J. D* **9**, 77 (1999).
- [35] See Supplemental Material at <http://link.aps.org/supplemental/10.1103/PhysRevB.90.195431> for the illustration of Hg-immersion-induced modifications of the CNTs on the apex of a metalized tip.
- [36] C. Kittel, *Introduction to Solid State Physics* (Wiley and Sons, Hoboken, NJ, 2004).
- [37] S. Datta, *Electronic Transport in Mesoscopic Systems* (Cambridge University Press, Cambridge, UK, 1995).
- [38] Z. L. Wang, P. Poncharal, and W. A. de Heer, *J. Phys. Chem. Solids* **61**, 1025 (2000).
- [39] C. Berger, P. Poncharal, Y. Yi, and W. de Heer, *J. Nanosci. Nanotechnol.* **3**, 171 (2003).
- [40] M. Kobylyko, *Phys. Rev. B* **90**, 195432 (2014).